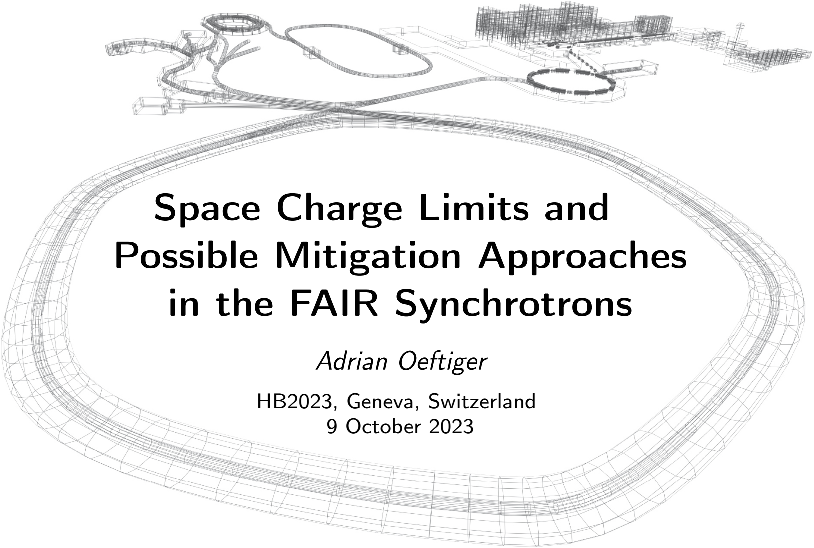

Space Charge Limits and Possible Mitigation Approaches in the FAIR Synchrotrons

Adrian Oeftiger

HB2023, Geneva, Switzerland
9 October 2023

FAIR Status

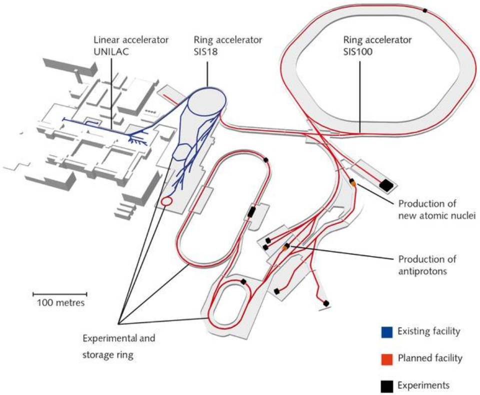

drone video of construction site ↗

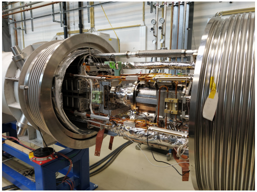

- string test of full SIS100 arc cell installed
- first SIS100 accelerator section to be installed in January 2024, IPAC'23 paper on SIS100 status ↗

Motivation

Facility for **A**ntiproton and **I**on **R**esearch

- SIS100: deliver high-intensity hadron beams

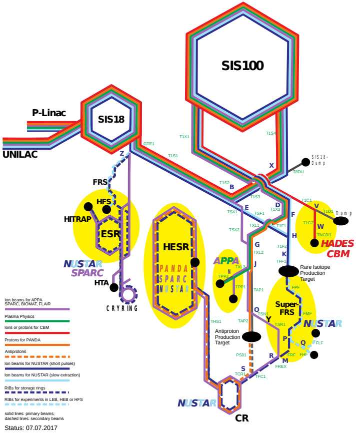

Figure: FAIR complex

Motivation

Facility for **A**ntiproton and **I**on **R**esearch

- SIS100: deliver high-intensity hadron beams
- crucial for performance: maintain beam quality during 1-sec injection plateau
- reference case: uranium U^{28+} beam
  - largest beam size vs. transverse aperture
  - space charge induced losses
    - ⇝ important: dynamic vacuum stability
    - ⟹ low-loss operation $< 5\%$!

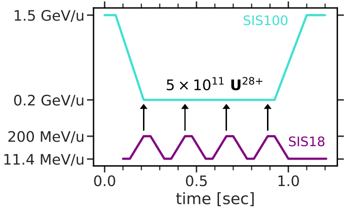

Figure: SIS18 to SIS100 transfer

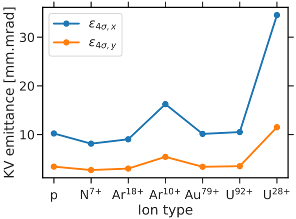

Figure: scaled beam sizes at 18 T m

Motivation

Facility for **A**ntiproton and **I**on **R**esearch

- SIS100: deliver high-intensity hadron beams
- crucial for performance: maintain beam quality during 1-sec injection plateau
- reference case: uranium U^{28+} beam
  - largest beam size vs. transverse aperture
  - space charge induced losses
    - ⇝ important: dynamic vacuum stability
    - ⟹ low-loss operation $< 5\%$!

key questions

- What is the maximum tolerable intensity at the space charge limit?
- How to increase the space charge limit?

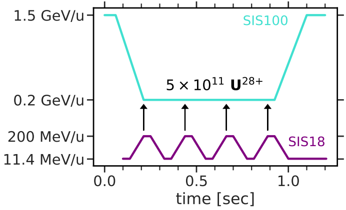

Figure: SIS18 to SIS100 transfer

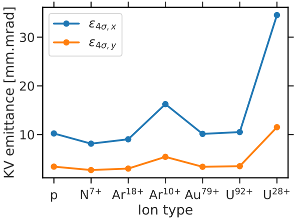

Figure: scaled beam sizes at 18 T m

Contents

Structure:

A. The Model

B. Betatron Resonances:
   - Intrinsic from Space Charge
   - External from Field Errors

C. Space Charge Limit

D. Mitigation Measures: Conventional & Novel
   - β-beat Compensation
   - Bunch Flattening
   - Pulsed Electron Lenses

A. The Model

Space Charge Modelling

Simulation model:

- track macro-particles (m.p.) through accelerator lattice & space charge kicks

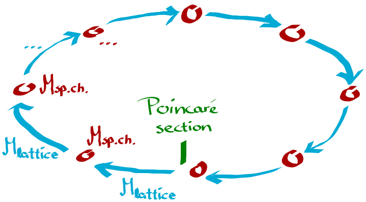

Figure: sketch of simulation model

Space Charge Modelling

Simulation model:

- track macro-particles (m.p.) through accelerator lattice & space charge kicks
- nonlinear 3D space charge (SC) models:
  - *self-consistent* ***PIC****:* particle-in-cell for open-boundary Poisson equation
  - *fixed frozen (****FFSC****):* constant field map independent of m.p. dynamics
  - (*adaptive frozen (****AFSC****):* field map scaled with m.p. distribution momenta)

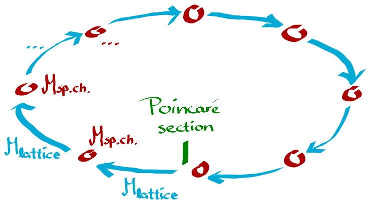

Figure: sketch of simulation model

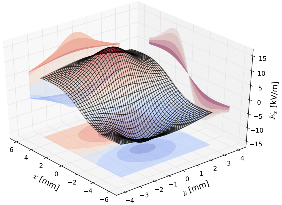

Figure: horizontal space charge field

Space Charge at SIS100 Accumulation

Maximum SC Tune Shift

$$\Delta Q_y^{SC} = -\frac{r_c \lambda_{max}}{\beta_0^2 \gamma_0^3} \oint \frac{ds}{2\pi} \frac{\beta_y(s)}{\sigma_y(s)(\sigma_x(s)+\sigma_y(s))}$$

r_c : classical ion radius λ_{max} : maximum line density

β_0 : speed in [c] γ_0 : Lorentz factor $\sigma_{x,y}$: local rms beam size

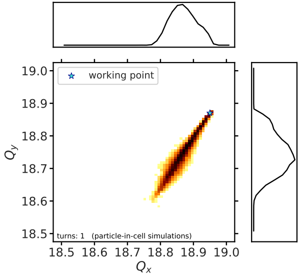

Hor. norm. rms emittance ϵ_x	5.9 mm mrad
Vert. norm. rms emittance ϵ_y	2.5 mm mrad
Rms bunch length σ_z	13.2 m
Bunch intensity N_0 of U^{28+} ions	6.25×10^{10}
Max. space charge ΔQ_y^{SC}	-0.30
Rms chromatic $Q'_{x,y} \cdot \sigma_{\Delta p/p_0}$	0.01
Synchrotron tune Q_s	4.5×10^{-3}
Kinetic energy	$E_{kin} = 200$ MeV/u
Relativistic β factor	0.568
Revolution frequency f_{rev}	157 kHz

B. Betatron Resonances

Only Space Charge

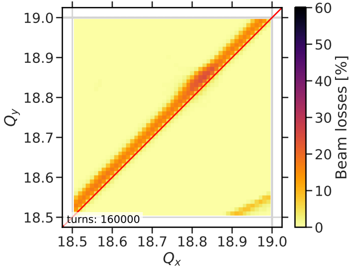

Figure: tune diagram of beam loss

Symmetric error-free SIS100 lattice:

- perfect dipole and quadrupole magnets
- exact symmetry of $S = 6$
- space charge → only source for resonances
- simulated for 160’000 turns = 1 second

$\Longrightarrow$ mainly Montague resonance visible

$\Longrightarrow$ absence of low-order structure resonances!

Only Space Charge

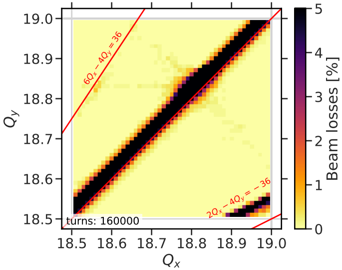

Figure: tune diagram of beam loss

Symmetric error-free SIS100 lattice:

- perfect dipole and quadrupole magnets
- exact symmetry of $S = 6$
- space charge → only source for resonances
- simulated for 160'000 turns = 1 second

⟹ mainly Montague resonance visible

⟹ absence of low-order structure resonances!

Montague resonance $2Q_x - 2Q_y = 0$:

- 4^{th}-order resonance
- intrinsically driven by space charge
- transverse emittance exchange for anisotropic beams

⟹ stopband always present around $Q_x \approx Q_y$ for SIS100 beams

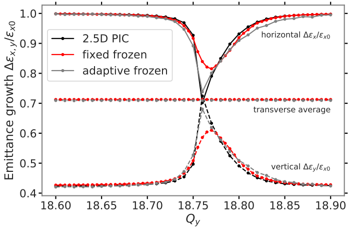

Figure: emittance exchange

Space charge model predictions:

– bad: "adaptive frozen" resolves full exchange but predicts too large stopband extent

+ good: "fixed frozen" reproduces stopband edges well!

Montague Resonance

Montague resonance $2Q_x - 2Q_y = 0$:

- 4^{th}-order resonance
- intrinsically driven by space charge
- transverse emittance exchange for anisotropic beams

$\Longrightarrow$ sto…
for …

Observation

"Fixed frozen" model much better suited than "adaptive frozen" to approximate realistic PIC when **identifying loss-free conditions**!

Space charge model predictions:

– bad: "adaptive frozen" resolves full exchange but predicts too large stopband extent

+ good: "fixed frozen" reproduces stopband edges well!

Figure: emittance exchange

Warm Quadrupoles

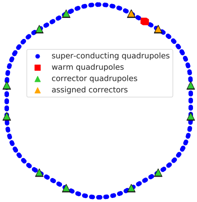

Figure: SIS100 quadrupole survey

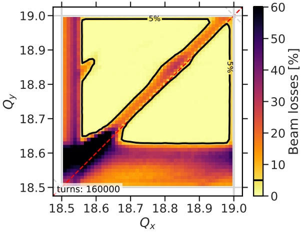

Figure: corrected warm quadrupoles

Real SIS100 lattice:

- 2 cold quadrupoles replaced by warm / normalconducting quadrupoles (radiation hardened, required in extraction region)
- breaking of $S = 6$ symmetry by gradient error

⟶ externally driven half-integer resonance

⟶ can be minimised by quadrupole correctors

⟹ FFSC reproduces PIC stopband edges!

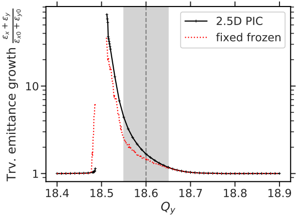

Field Error Model

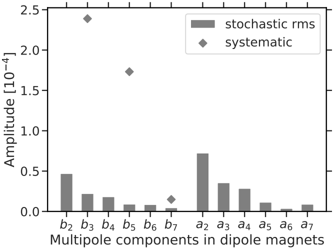

Figure: dipole magnets

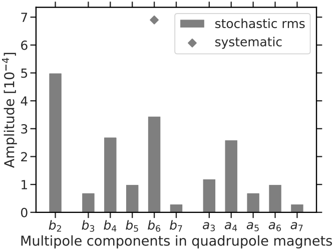

Figure: quadrupole magnets

Field error model extracted from cold bench measurements of magnet units:

- stochastic amplitudes drive non-systematic resonances
- random number sequence → multipole errors for every dipole and quadrupole magnet

quadrupole model displayed here corresponds to PRAB paper version (based on stamped FoS), see GSI-2021-00450 report ↗ for model based on series production and its comparison

Field Error Model from Beam

HB'23 talk on Wednesday, C. Caliari on "Deep Lie Map Network" ↗:

- machine learning approach: train linear & nonlinear field errors on kick turn-by-turn data
- start from model lattice, learn error multipoles k·L

⟹ effective lattice to better reproduce machine behaviour

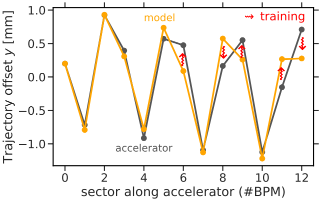

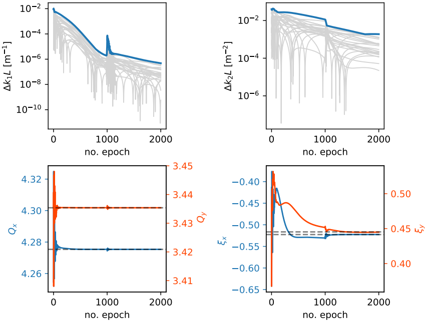

Figure: learning of quadrupole & sextupole errors

Full Model with Space Charge

Linear and nonlinear resonances driven by magnet field errors. Resonance condition without space charge:

$$mQ_x + nQ_y = p \qquad \text{for} \quad m, n, p \in \mathbb{Z}$$

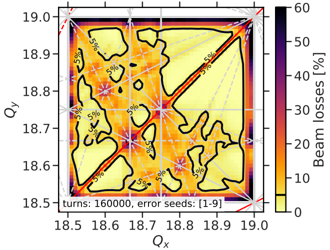

Figure: no space charge

Full Model with Space Charge

Linear and nonlinear resonances driven by magnet field errors. Resonance condition without space charge:

$$mQ_x + nQ_y = p \qquad \text{for} \quad m, n, p \in \mathbb{Z}$$

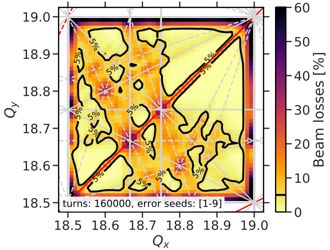

Figure: no space charge

include $\Longrightarrow$ SC

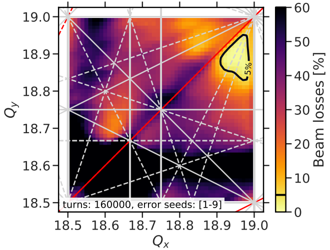

Figure: with fixed frozen space charge

$\longrightarrow$ SC broadens existing resonance stopbands

$\Longrightarrow$ optimal working point area around $(Q_x, Q_y) = (18.95, 18.87)$

Validation with Self-consistent PIC

Self-consistent PIC simulations:

- ✓ validated Montague resonance
- ✓ validated half-integer resonance
- ⟶ now validate full error model FFSC predictions for beam loss

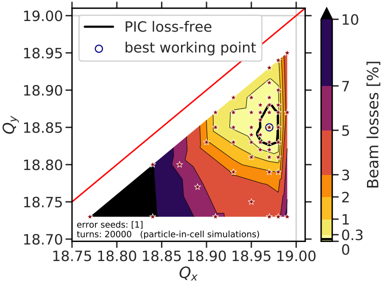

Figure: self-consistent PIC simulations

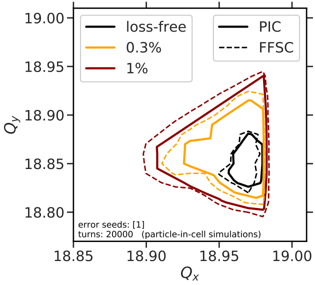

Figure: comparison between SC models

note: PIC simulations take 2 days (on NVIDIA V100 GPU) vs. FFSC simulations with 7 min (on 16 CPU cores, HPC AMD)

C. Space Charge Limit

dynamic definition of space charge limit

reached when loss-free working point area vanishes

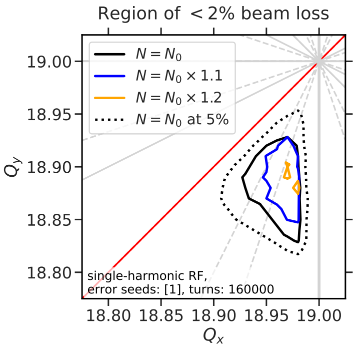

Figure: low-loss area for increasing N

Keeping all beam parameters identical, increasing N:

$\Longrightarrow$ U^{28+} space charge limit at **120%** of nominal bunch intensity N_0:

$$\max \left| \Delta Q_y^{SC} \right| = 0.36$$

D. Mitigation Measures: Conventional & Novel

Correction of β-beat

Two sources of β-beat (gradient error):

- warm quadrupoles: uncorrected = 2%

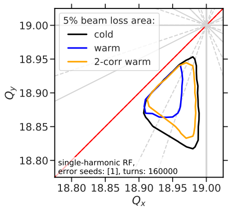

(a) low-loss area with warm quads

Correction of β-beat

Two sources of β-beat (gradient error):

- warm quadrupoles: uncorrected = 2%
- distributed b_2: $\approx 0.5\%$

$\Longrightarrow$ below $b_2 = 10$ units: no significant effect on low-loss area size

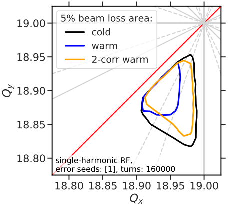

(a) low-loss area with warm quads

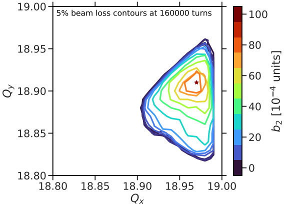

(b) low-loss area with b_2

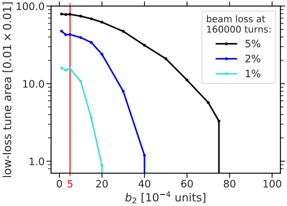

(c) size of low-loss area vs. b_2

A Word on Coherent Stability

For SIS100, space charge parameter $q = \Delta Q_y^{SC}/2Q_s \approx 33$ at design $N = N_0$:

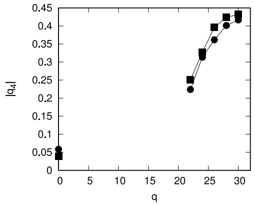

Figure 4: Results of the simulations scans for the $k = 1$ mode: stability thresholds of the octupole power in a dependency from the space-charge parameter q. The circles are for the octupole polarity $q_4 > 0$, the squares are for the octupole polarity $q_4 < 0$.

(a) Required octupole strength for stabilisation of single-bunch resistive-wall instability [V. Kornilov, IPAC'23] ↗

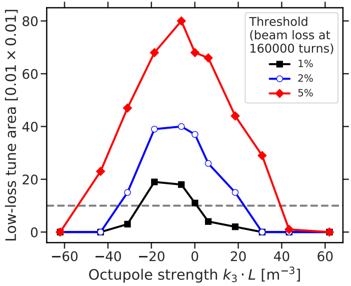

(b) Incoherently tolerable octupole strengths

- octupole current of $k_3 L = 35\,\mathrm{m}^{-3}$ corresponds to $q_4 = 0.55$.

⟹ single-bunch stability through Landau damping from octupoles, transverse feedback system required for coupled-bunch stability

Double-harmonic RF

Add $h = 20$ harmonic in bunch lengthening mode:

$$V_{h=20} = V_{h=10}/2$$

$\implies$ obtain flattened bunches with reduced line density at 80% of nominal $\lambda_{\max}$.

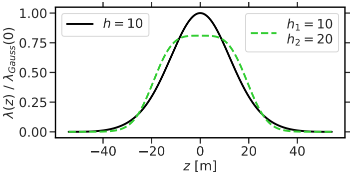

Figure: rms-equivalent line densities

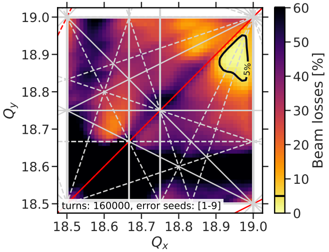

Figure: single-harmonic RF

flatten
$\Longrightarrow$
bunch

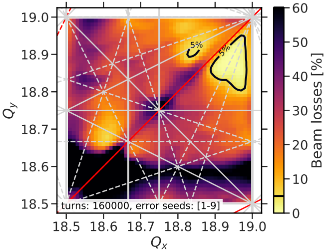

Figure: double-harmonic RF

SC Limit with Double-harmonic RF

Increasing N for double-harmonic RF:

- find space charge limit at **150%** of nominal intensity N_0

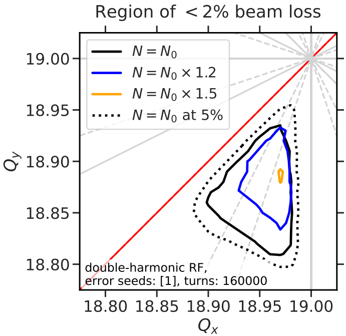

Figure: low-loss area for increasing N

Novel: Pulsed Electron Lenses

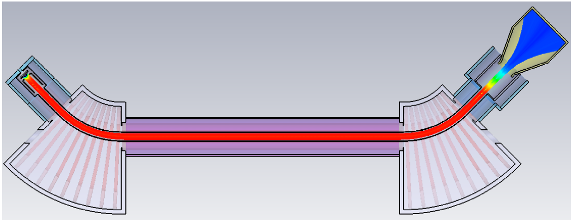

Figure: e-lens model for SIS18 [K. Schulte-Urlichs et al., IPAC'22] ↗

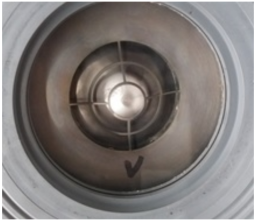

Figure: Modulation grid.

Short insertion (here $L = 3.36\,\mathrm{m}$) with co-propagating electron beam:

- transversely homogeneous distribution
- longitudinally modulated to match ion bunch profile

⟶ compensate longitudinal dependency of space charge

⟹ **suppress periodic resonance crossing**

⟶ additionally provide strong Landau damping for head-tail modes:
V. Gubaidulin et al., PRAB 25, 084401 (2022) ↗ [tbc with strong SC]

Tune Footprint vs. E-Lens Compensation

Some n_{el} e-lenses with I_e current and rms beam size σ_e provide tune shift:

$$\Delta Q_y^e = \frac{1}{4\pi} \sum_{k=1}^{n_{el}} \beta_y(s_k) \frac{r_c}{Ze} \frac{I_e}{\sigma_e^2 \gamma_0} \frac{1-\beta_e\beta_0}{\beta_e} \frac{L}{\beta_0 c}$$

Define linear compensation degree (for Gaussian bunches $\Delta Q^{KV} = \Delta Q^{SC}/2$):

$$\alpha \doteq \frac{\Delta Q^e}{|\Delta Q^{KV}|}$$

Remarks:

- dipole tune increases with

$$\Delta Q_{dip} = \alpha \cdot \Delta Q^e$$

- without chroma, $\alpha = 0.5$ yields smallest tune spread!

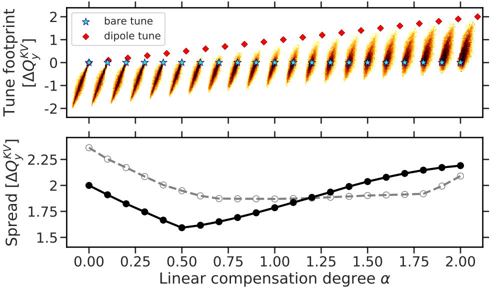

Figure: Gaussian bunch, tune footprint vs. e-lens strength (black: $\Delta p/p_0 = 0$, grey: with natural chromatic detuning)

Optimal E-Lens Configuration

In SIS100 with natural chromaticity:

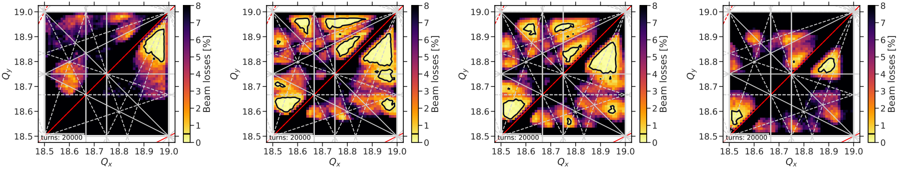

(a) $\alpha = 0$ (b) $\alpha = 0.5$ (c) $\alpha = 0.7$ (d) $\alpha = 1$

Figure: FAIR design intensity $N = N_0$ with $n_{el} = 3$ pulsed e-lenses.

- optimal choice of α depends on nearby resonances
  $\Longrightarrow$ depends on particularities of synchrotron
- SIS100: at low $n_{el} \leq 6$, $\alpha = 0.5$ optimal vs. high $n_{el} > 6$, $\alpha = 0.7$ better

SC Limit with Pulsed E-Lenses

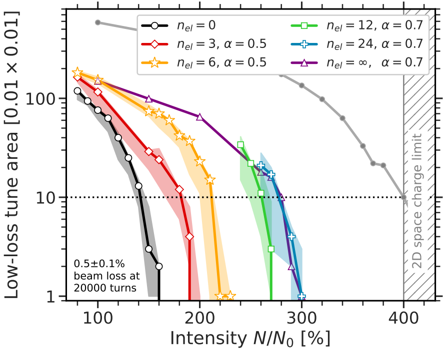

Figure: low-loss area for increasing N

Table: SC limit with electron lenses.

Number n_{el}	SC limit	Gain
0	$1.4 \cdot N_0$	100%
3	$1.8 \cdot N_0$	130%
6	$2.1 \cdot N_0$	150%
12	$2.6 \cdot N_0$	185%
$24, \infty$	$2.8 \cdot N_0$	200%

Remarks:

- SC limit scales well
- $n_{\text{el}} = 24$ case saturates gain
- theoretical 2D limit ($Q_s = 0$, no e-lenses) = by construction no periodic resonance crossing
  - $\Longrightarrow$ reached after $n_{\text{el}} = 24, \infty$

Involved Publications

PHYSICAL REVIEW ACCELERATORS AND BEAMS **25,** 054402 (2022)

Simulation study of the space charge limit in heavy-ion synchrotrons

Adrian Oeftiger,[1,*] Oliver Boine-Frankenheim,[1,2] Vera Chetvertkova,[1]
Vladimir Kornilov,[1] Dmitrii Rabusov,[2] and Stefan Sorge[1]

[1]*GSI Helmholtzzentrum für Schwerionen*
[2]*Technische Universität Darmsta*

(Received 5 November 2(

Pulsed Electron Lenses for Space Charge Mitigation

Adrian Oeftiger[1,*] and Oliver Boine-Frankenheim[1,2]

[1]*GSI Helmholtzzentrum für Schwerionenforschung GmbH, Planckstrasse 1, 64291 Darmstadt, Germany*
[2]*Technische Universität Darmstadt, Schlossgartenstrasse 8, 64289 Darmstadt, Germany*

(Dated: October 5, 2023)

Jinst

Published by IOP Publishing for Sissa Medialab

Received: *February 15, 2021*
Accepted: *February 22, 2021*
Published: *March 31, 2021*

ICFA Beam Dynamics Newsletter#81 —
Electron Lenses for Modern and Future Accelerators

Pulsed electron lenses for space charge compensation in the FAIR synchrotrons

S. Artikova,[a] O. Boine-Frankenheim,[a,b,*] O. Meusel,[c] A. Oeftiger,[a] D. Ondreka,[a]
K. Schulte-Urlichs[a] and P. Spiller[a]

Nuclear Inst. and Methods in Physics Research, A 1040 (2022) 167290

Contents lists available at ScienceDirect

Nuclear Inst. and Methods in Physics Research, A

journal homepage: www.elsevier.com/locate/nima

ELSEVIER

Characterization and minimization of the half-integer stop band with space charge in a hadron synchrotron

Check for updates

Dmitrii Rabusov[a,*], Adrian Oeftiger[b], Oliver Boine-Frankenheim[a,b]

[a] *Technische Universität Darmstadt, Schlossgartenstr. 8, 64289 Darmstadt, Germany*
[b] *GSI Helmholtzzentrum für Schwerionenforschung GmbH, Planckstr. 1, 64291 Darmstadt, Germany*

Conclusion

Summary:

- identified **optimal tune area** in SIS100 around $(Q_x, Q_y) = (18.95, 18.87)$
- explored **space charge limit**: $\max\left|\Delta Q_y^{\mathrm{SC}}\right| = 0.36$
  - nominal SIS100: +20% intensity
  - double-harmonic RF: +50% intensity
  - 3 pulsed electron lenses: +70..80% intensity
- FAIR start planned in 2028 with "Early Science" programme

Conclusion

Summary:

- identified **optimal tune area** in SIS100 around $(Q_x, Q_y) = (18.95, 18.87)$
- explored **space charge limit**: $\max \left| \Delta Q_y^{SC} \right| = 0.36$
  - nominal SIS100: +20% intensity
  - double-harmonic RF: +50% intensity
  - 3 pulsed electron lenses: +70..80% intensity
- FAIR start planned in 2028 with "Early Science" programme

take-home messages

- fixed frozen SC model fast & validated tool to identify resonance-free tunes
- dynamic space charge limit: find based on tolerable loss & emittance growth
- pulsed electron lenses: optimum configuration for space charge mitigation

Thank you for your attention!

Acknowledgements:

GSI: O. Boine-Frankenheim, V. Chetvertkova, V. Kornilov, D. Rabusov, S. Sorge, D. Ondreka, A. Bleile, V. Maroussov, C. Roux, K. Sugita

CERN: R. de Maria, G. Iadarola, M. Schwinzerl

Grand Overview Tune Diagrams

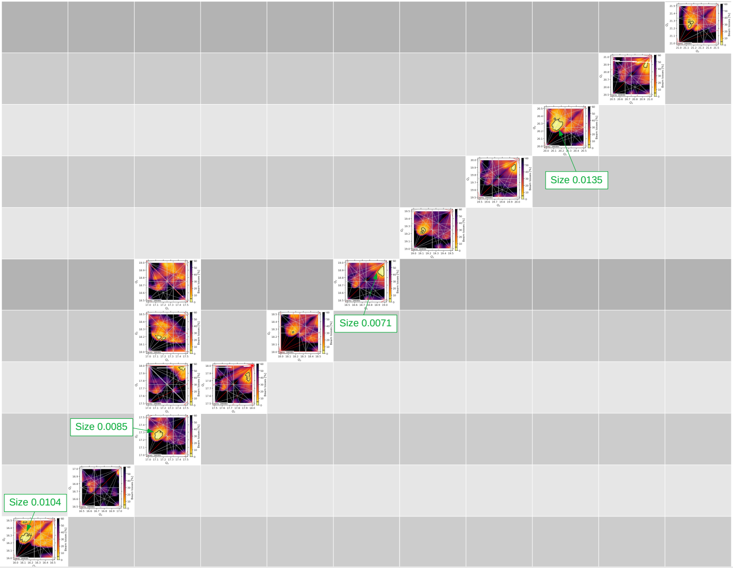

... the new GPU cluster ...

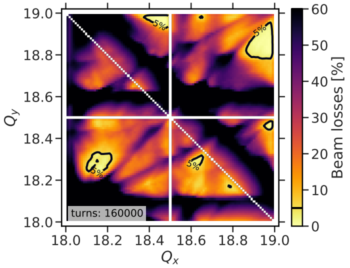

Figure: GPU simulation results for latest magnet field error model

Thanks to GSI's new high-performance GPU cluster in Green Cube:

- 400 GPU cards of today's most performant model (AMD Radeon Instinct MI100)
- even faster simulations, larger tune scans in shorter times

$\Longrightarrow$ following up magnet series production and doublet assembly

Why Homogeneous E-lenses?

O. Boine-Frankenheim and W. Stem, NIM A 896 (2018) 122–128 ↗:

- transversely Gaussian distributed pulsed e-lenses drive **strong systematic nonlinear resonances**

⟹ configuration with low number of Gaussian e-lenses not feasible

Their 2D simulation results with self-consistent PIC:

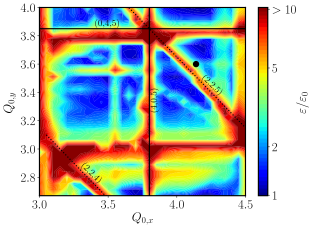

Fig. 8. 2D PIC tune scan for $N_e = 3$, $\Delta Q_{x,y} = -0.2/0.4$ and $\alpha = 0.5$ for a Gaussian electron beam.

(a) Gaussian pulsed e-lens

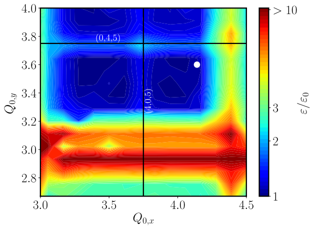

Fig. 9. 2D PIC tune scan for $N_e = 3$, $\Delta Q_{x,y} = -0.2/0.4$ and $\alpha = 0.5$ for a homogeneous electron beam.

(b) Homogeneous pulsed e-lens

Location of E-lenses

Electron lenses are placed in locations

- of equal $\beta_x = \beta_y$ (then electron pulse aspect ratio = ion beam for balanced compensation in both planes)
- in the straight section (avoid dispersion!)

$\Longrightarrow$ 4 possible locations per each sector (out of 6)

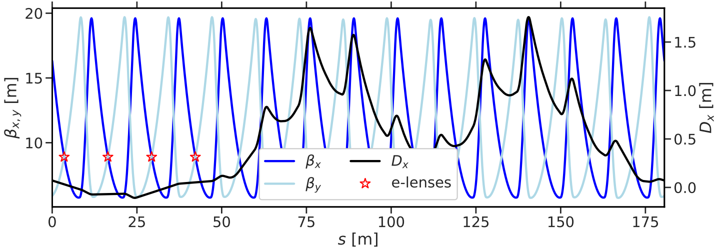

Figure: Optics functions for 1 sector in SIS100

SC-Limit Dependency on α

For $\alpha = 0.5$, SC limit with 24 e-lenses reached at $N = 2.6 \cdot N_0$.

⟶ can we do better for other α?

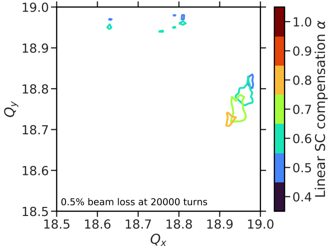

(a) loss boundaries vs. α

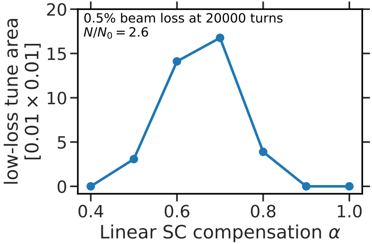

(b) low-loss tune area vs. α

Figure: Finding optimal α at $N = 2.6 \cdot N_0$

⟹ yes! $\alpha = 0.7$ looks much better at higher $n_{el} > 6$!

Cross-check with PIC

For 6 e-lenses at $N = 2 \cdot N_0$ and $\alpha = 0.5$, compare FFSC results to PIC:

FFSC (20k turns)

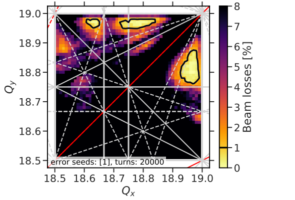

PIC (1k turns)

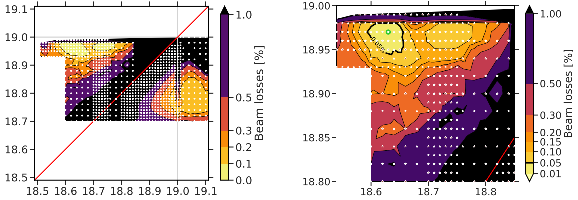

$\longrightarrow$ no surprises (coherent resonances etc.), low-loss tune areas match

$\Longrightarrow$ FFSC results for SC limit validated!

Relevant Field Error Orders

Major resonances confining low-loss area:

- top left: Montague resonance
- right: integer resonance $Q_x = 19$
- bottom: higher-order resonances

Simulations with reduced field error model:

- identify sextupole and octupole orders $n = 3, 4$ as main limitation towards low Q_y

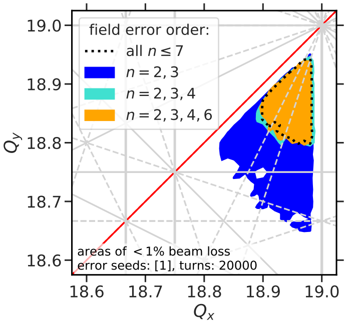

Figure: low-loss tune areas vs. multipole order

Emittance Growth at Low-loss Area

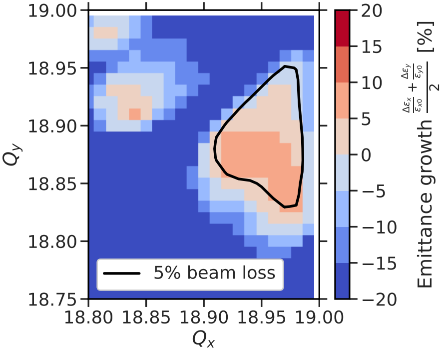

Figure: with space charge, emittance growth

PIC Results for Best Working Point

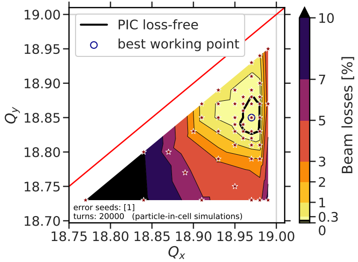

Figure: tune diagram with self-consistent PIC simulations

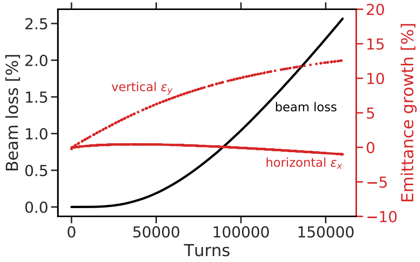

Figure: best working point $(Q_x, Q_y) = (18.97, 18.85)$

$\Longrightarrow$ high-resolution[1] PIC results indeed show $\approx 2.5\% < 5\%$ beam loss in identified area

[1]using 20×10^6 macro-particles in simulation such that resonance-free ideal lattice gives 0% beam loss, 160 000 turns compute for $\approx$ weeks on NVIDIA V100 GPU

Comparison 2.5D to 3D PIC

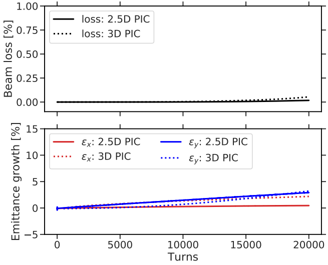

Figure: good working point $(Q_x, Q_y) = (18.97, 18.85)$

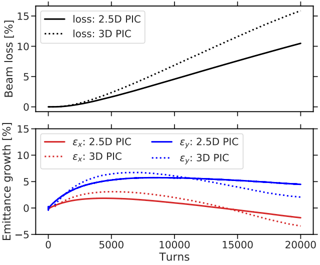

Figure: lossy working point $(Q_x, Q_y) = (18.84, 18.73)$

$\Longrightarrow$ 3D confirms 2.5D PIC results

Adaptive Frozen SC (AFSC) Model

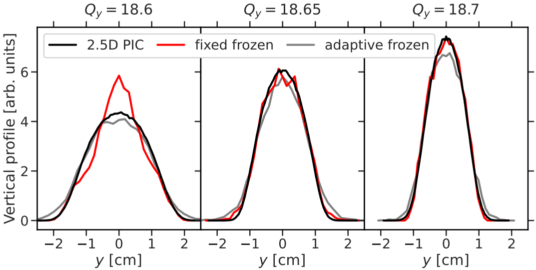

Observations from vertical beam profiles throughout half-integer stopband:

- black PIC = "truth"
- left two panels: AFSC ≈ PIC, only for strongly resonance-affected WPs
- BUT right panel: FFSC ≈ PIC, at edge of stopband

⟹ FFSC better suited than AFSC to reproduce stopband edges!

Why no Chromaticity Correction?

SIS100 lattice: optimised for dynamic vacuum stability with intermediately-charged heavy ions

- suppress dispersion where possible
  - ⟶ cryo-catchers where dispersion $\Longrightarrow$ removal of charge-stripped ions
- require strong sextupole current for full chromaticity correction $Q'_{x,y} = 0$
- at injection: large beam sizes vs. restricted dynamic aperture

Simulation results without space charge:

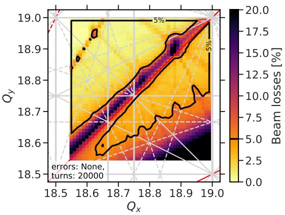

(a) just sextupoles, no field errors

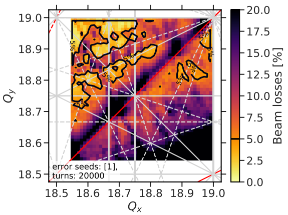

(b) sextupoles + field errors

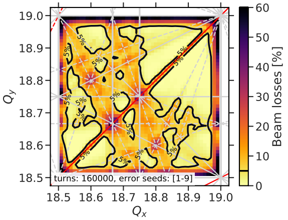

(c) no sextupoles, just field errors

Beta-Beating from Warm Quadrupoles

Beta-beating with and without adjacent quadrupole correctors at $Q_{x,y} = (18.84, 18.73)$:

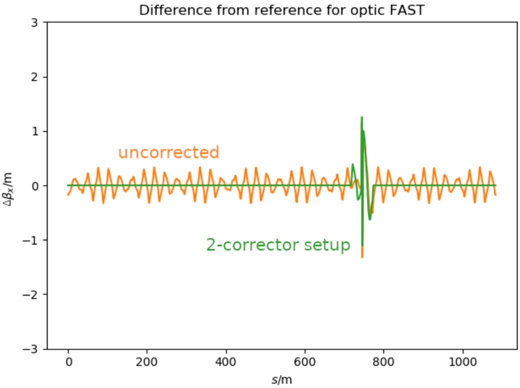

Figure: β-beat around SIS100 [courtesy D. Ondreka]

Harmonics with 2 Warm Quadrupoles

Fourier spectrum of single-turn envelope motion with space charge:

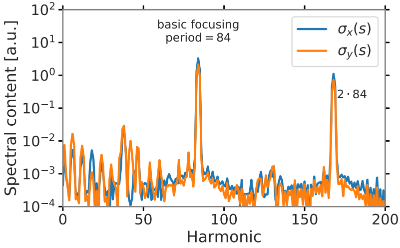

(a) Only cold quadrupoles

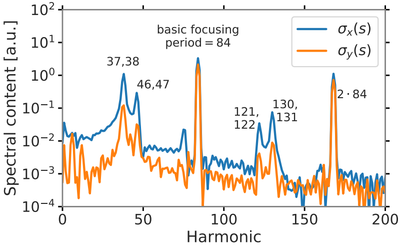

(b) With 2 warm quadrupoles

Observations:

- strong harmonics emerge at $2 \cdot Q_{x,y} \approx 38$ for half-integer resonance

Half-integer Resonance vs. SC

Nuclear Inst. and Methods in Physics Research, A 1040 (2022) 167290

Contents lists available at ScienceDirect

Nuclear Inst. and Methods in Physics Research, A

journal homepage: www.elsevier.com/locate/nima

Characterization and minimization of the half-integer stop band with space charge in a hadron synchrotron

Dmitrii Rabusov [a,*], Adrian Oeftiger [b], Oliver Boine-Frankenheim [a,b]

[a] Technische Universität Darmstadt, Schlossgartenstr. 8, 64289 Darmstadt, Germany

[b] GSI Helmholtzzentrum für Schwerionenforschung GmbH, Planckstr. 1, 64291 Darmstadt, Germany

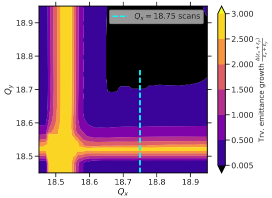

Figure: emittance growth in 2D tune diagram

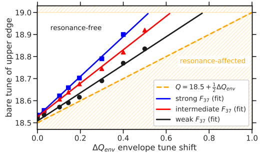

Figure: space charge limit for Gaussian bunches

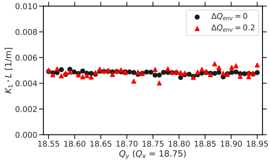

Figure: correction independent of space charge

Half-integer Resonance vs. SC

Nuclear Inst. and Methods in Physics Research, A 1040 (2022) 167290

Contents lists available at ScienceDirect

Nuclear Inst. and Methods in Physics Research, A

journal homepage: www.elsevier.com/locate/nima

Characterization and minimization of the half-integer stop band with space charge in a hadron synchrotron

Dmitrii Rabusov [a,*], Adrian Oeftiger [b], Oliver Boine-Frankenheim [a,b]

[a] Technische Universität Darmstadt, Schlossgartenstr. 8, 64289 Darmstadt, Germany
[b] GSI Helmholtzzentrum für Schwerionenforschung GmbH, Planckstr. 1, 64291 Darmstadt, Germany

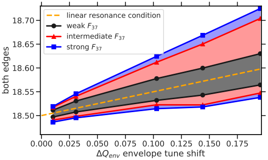

Figure: coasting beam stopband edges vs. space charge

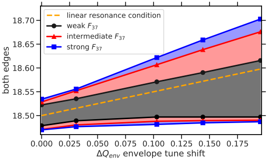

Figure: bunched beam stopband edges vs. space charge

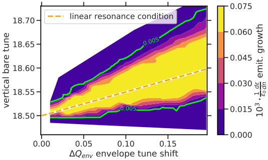

Figure: choose a threshold

Half-integer Resonance

Vertical half-integer stopband:

- no space charge, without $\Delta p/p_0$: $\delta Q_{\text{stopband}} = 0.023$
- no space charge, with $\Delta p/p_0$: $\delta Q_{\text{stopband}} \sim 0.1$
- incl. space charge: $\delta Q_{\text{stopband}} \sim 0.25$

$\Longrightarrow$ fixed frozen SC model reproduces stopband edges from PIC

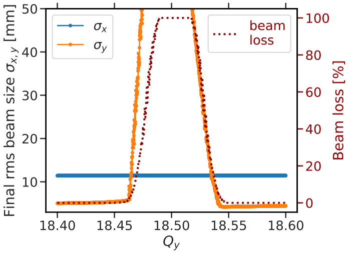

Figure: no space charge

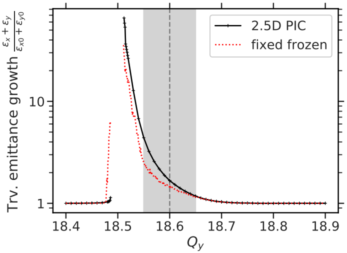

Figure: with space charge

Half-integer without SC but with Chroma

Chromaticity critical for half-integer width! ($Q'_y = -22.5$ and $\sigma_{\Delta p/p_0} = 0.5 \times 10^{-3}$)

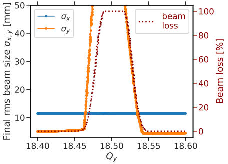

(a) full momentum spread

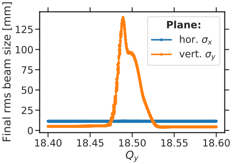

(b) half momentum spread

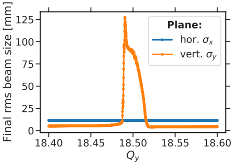

(c) 10% momentum spread

$\Longrightarrow$ for vanishing $\sigma_{\Delta p/p_0} \to 0$, simulated width matches analytical $\Delta Q_{1/2} = 0.023$

Half-integer without SC but with Chroma

Chromaticity critical for half-integer width! ($Q'_y = -22.5$ and $\sigma_{\Delta p/p_0} = 0.5 \times 10^{-3}$)

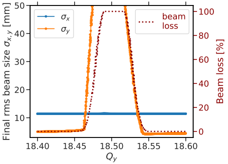

(a) full momentum spread

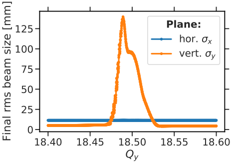

(b) half momentum spread

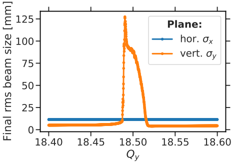

(c) 10% momentum spread

⟹ for vanishing $\sigma_{\Delta p/p_0} \to 0$, simulated width matches analytical $\Delta Q_{1/2} = 0.023$

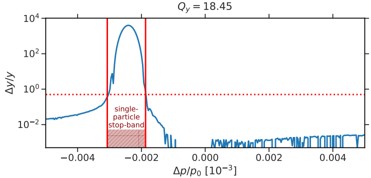

Figure: shifted single-particle stopband

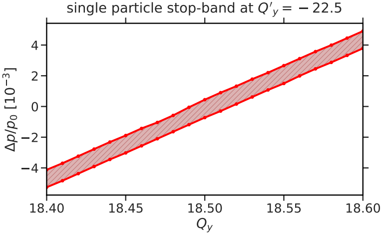

Half-integer without SC but with Chroma

Chromaticity critical for half-integer width! ($Q'_y = -22.5$ and $\sigma_{\Delta p/p_0} = 0.5 \times 10^{-3}$)

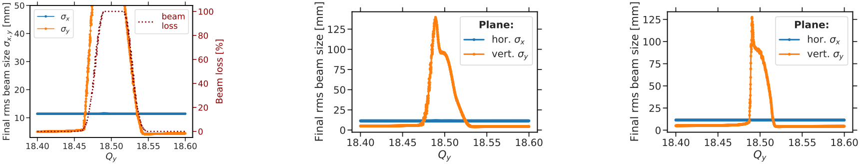

(a) full momentum spread (b) half momentum spread (c) 10% momentum spread

$\Longrightarrow$ for vanishing $\sigma_{\Delta p/p_0} \to 0$, simulated width matches analytical $\Delta Q_{1/2} = 0.023$

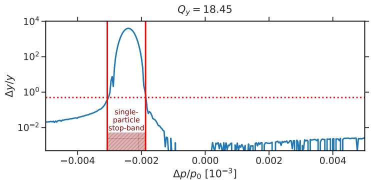

Figure: shifted single-particle stopband

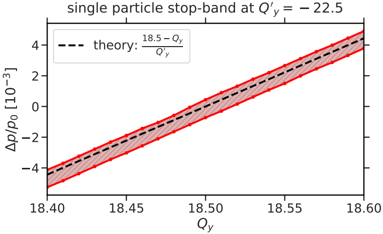

Half-integer without SC but with Chroma

Chromaticity critical for half-integer width! ($Q'_y = -22.5$ and $\sigma_{\Delta p/p_0} = 0.5 \times 10^{-3}$)

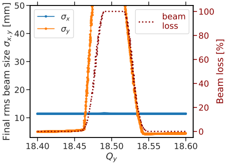

(a) full momentum spread

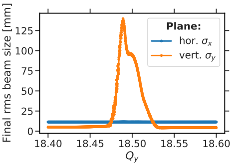

(b) half momentum spread

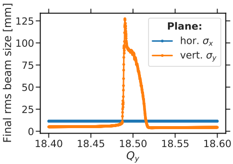

(c) 10% momentum spread

⟹ for vanishing $\sigma_{\Delta p/p_0} \to 0$, simulated width matches analytical $\Delta Q_{1/2} = 0.023$

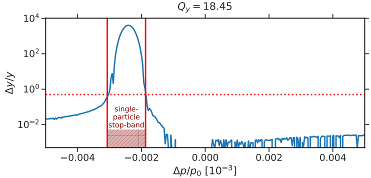

Figure: shifted single-particle stopband

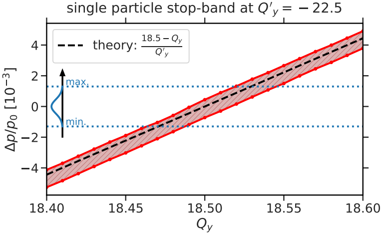

Half-integer without SC but with Chroma

Chromaticity critical for half-integer width! ($Q'_y = -22.5$ and $\sigma_{\Delta p/p_0} = 0.5 \times 10^{-3}$)

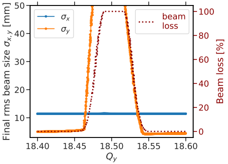

(a) full momentum spread

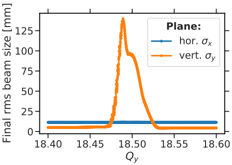

(b) half momentum spread

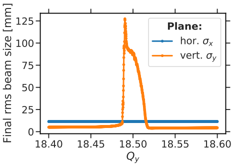

(c) 10% momentum spread

$\Longrightarrow$ for vanishing $\sigma_{\Delta p/p_0} \to 0$, simulated width matches analytical $\Delta Q_{1/2} = 0.023$

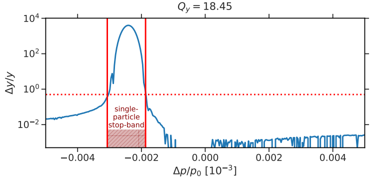

Figure: shifted single-particle stopband